Pharm Res (2015) 32:260–274
DOI 10.1007/s11095-014-1460-x

RESEARCH PAPER

Physiology-Based IVIVE Predictions of Tramadol from *in Vitro* Metabolism Data

Huybrecht T'jollyn • Jan Snoeys • Pieter Colin • Jan Van Bocxlaer • Pieter Annaert • Filip Cuyckens • An Vermeulen • Achiel Van Peer • Karel Allegaert • Geert Mannens • Koen Boussery

Received: 16 April 2014 / Accepted: 2 July 2014 / Published online: 22 July 2014

ABSTRACT

Purpose To predict the tramadol *in vivo* pharmacokinetics in adults by using *in vitro* metabolism data and an *in vitro-in vivo* extrapolation (IVIVE)-linked physiologically-based pharmacokinetic (PBPK) modeling and simulation approach (Simcyp®).

Methods Tramadol metabolism data was gathered using metabolite formation in human liver microsomes (HLM) and recombinant enzyme systems (rCYP). Hepatic intrinsic clearance ($CLint_H$) was (i) estimated from HLM corrected for specific CYP450 contributions from a chemical inhibition assay (model 1); (ii) obtained in rCYP and corrected for specific CYP450 contributions by study-specific inter-system extrapolation factor (ISEF) values (model 2); and (iii) scaled back from *in vivo* observed clearance values (model 3). The model-predicted clearances of these three models were evaluated against observed clearance values in terms of relative difference of their geometric means, the fold difference of their coefficients of variation, and relative CYP2D6 contribution.

Results Model 1 underpredicted, while model 2 overpredicted the total tramadol clearance by −27 and +22%, respectively. The CYP2D6 contribution was underestimated in both models 1 and 2. Also, the variability on the clearance of those models was slightly underpredicted. Additionally, blood-to-plasma ratio and hepatic uptake factor were identified as most influential factors in the prediction of the hepatic clearance using a sensitivity analysis.

Conclusion IVIVE-PBPK proved to be a useful tool in combining tramadol's low turnover *in vitro* metabolism data with system-specific physiological information to come up with reliable PK predictions in adults.

KEY WORDS clearance mechanisms · *in vitro* metabolism · IVIVE · PBPK

ABBREVIATIONS

PBPK	Physiologically-based pharmacokinetics
IVIVE	*In vitro-in vivo* extrapolation
CLint	Intrinsic clearance
HLM	Human liver microsomes
rCYP	Recombinant CYP450 enzyme systems
ISEF	Inter-system extrapolation factor
ODT	O-desmethyltramadol
NDT	N-desmethyltramadol
NODT	N,O-didesmethyltramadol

INTRODUCTION

Tramadol is a centrally acting analgesic drug with weak opioid activity and has an established use in the clinical setting (1). Tramadol is metabolized by different cytochrome P450 enzymes (CYP450), of which CYP3A4 and CYP2D6 are deemed to be the most important ones (2,3) (Fig. 1). CYP3A4 governs the metabolism of about 50% of clinically used drugs and is characterized by large interindividual variability (4). Also for CYP2D6 genetic polymorphisms have been described that can lead to large interindividual variation in substrate pharmacokinetics (5). Tramadol, which inhibits

H. T'jollyn • P. Colin • J. Van Bocxlaer • A. Vermeulen • K. Boussery (✉)
Laboratory of Medical Biochemistry and Clinical Analysis, Faculty of Pharmaceutical Sciences, Ghent University, Ottergemsesteenweg 460 9000 Ghent Belgium
e-mail: koen.boussery@ugent.be

J. Snoeys • F. Cuyckens • A. Vermeulen • A. Van Peer • G. Mannens
Division of Janssen Pharmaceutica NV, Janssen Research and Development, Turnhoutseweg 30 2340 Beerse Belgium

P. Annaert
Drug Delivery and Disposition, KU Leuven Department of Pharmaceutical and Pharmacological Sciences, O&N2, Herestraat 49-box 921 3000 Leuven Belgium

K. Allegaert
Department of Development and Regeneration, KU Leuven and Neonatal Intensive Care Unit, University Hospitals Leuven, 3000 Leuven Belgium

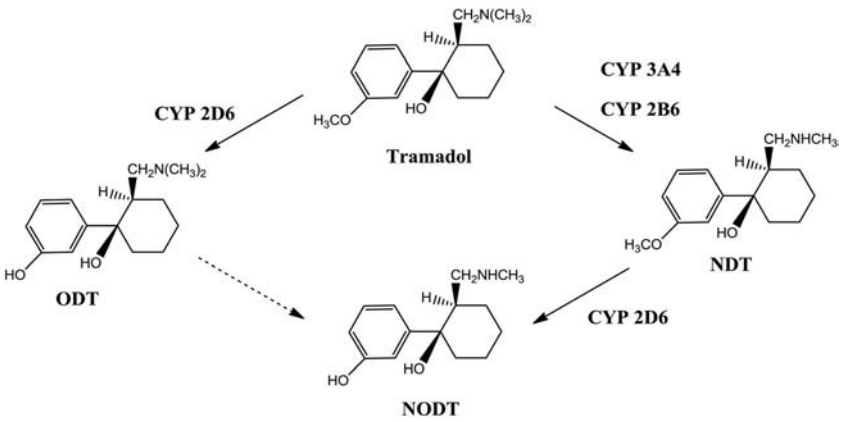

Fig. 1 Tramadol CYP450 metabolism pathways (O-desmethyltramadol (ODT); N-desmethyltramadol (NDT); NODT (N,O-didesmethyltramadol)).

neuronal uptake of norepinephrine and serotonine, is bioactivated by CYP2D6 to its O-demethylated metabolite that has 300 times more affinity for the μ-opioid receptor than tramadol (1). Therefore, CYP2D6 activity and metabolizer status may have implications on the pharmacokinetics and on the extent of μ-opioid effect after administration of this drug (6,7). The above described metabolism properties make this drug an interesting compound to study the performance of bottom-up physiologically-based pharmacokinetic (PBPK) modeling, relying on *in vitro* drug metabolism kinetics to predict *in vivo* pharmacokinetics.

In the past, the use of PBPK models was limited due to their complexity and high computational requirements. Therefore, simpler, empirical methods such as sums of exponentials and compartmental models, were commonly chosen to 'describe' the (plasma) concentration-time profiles (8). PBPK models represent the studied organism as a closed circulatory system in which organs and different tissues make up the physiologically relevant compartments, interconnected by the blood circulation, independent of the drug under investigation (9). In order to make compound-specific PBPK predictions, compound-specific information, such as molecular descriptors logP, pKa, molecular weight (Mw), and *in vitro* measured values intrinsic clearance (CLint), Km, Vmax, blood-plasma ratio, fraction unbound in plasma have to be provided (10). The mechanistic extrapolation of *in vitro* pharmacokinetic data to *in vivo* is the so-called bottom-up IVIVE-linked PBPK approach and allows to predict first-in-man pharmacokinetic exposure, anticipate major drug-drug interactions, and predict drug clearance in subject populations at risk (e.g., renal/hepatic impaired, pediatric populations) (11,12). Furthermore, this bottom-up PBPK approach is able to *a priori* identify disposition covariates of a new drug candidate through *in vitro* investigation, and can provide mechanistic insight in the observed absorption, distribution, metabolism, and excretion properties of the studied compound. Nevertheless, the classical 'top-down' approach will remain a vital complementary tool to adequately describe the observed data obtained in clinical studies (13).

In IVIVE, it is extremely important that the metabolic enzyme kinetic data are obtained under optimal conditions to build a robust quantitative PBPK model. Intrinsic metabolic drug clearance values can be determined by using metabolite formation or substrate depletion assays. In substrate depletion assays, the *in vitro* half-life of the drug is determined (14) and at least 20% compound turnover is required for analytical reasons. In such assays, especially for low clearance drugs, long incubation times and relatively high protein concentrations are needed. This may lead to issues such as loss in enzyme activity over time, end product inhibition, and binding problems, thus preventing reliable prediction of drug clearance. However, other methods (such as the hepatocyte relay method) are now available that allow accurate and precise measurement of compounds with low *in vitro* turnover (15). Metabolite formation assays use initial rates, enabling the use of shorter incubation times and lower protein concentrations. However, reference standards for metabolites are needed for the bioanalysis. Underprediction of clearance can occur if not all metabolic pathways are accounted for (16). As an alternative, formation of all metabolites originating from a parent compound can be studied by using a radiolabel in the incubation experiments.

In this manuscript we present an extended case study on the IVIVE-PBPK prediction of tramadol. The hepatic intrinsic clearance ($CLint_H$) was estimated using three different clearance models: $CLint_H$ from human liver microsomal (HLM) metabolism data corrected for specific CYP450 contributions from a chemical inhibition assay (model 1, HLM model); $CLint_H$ obtained from recombinant enzyme systems corrected for specific CYP450 contributions by study-specific intersystem extrapolation factor (ISEF) values (model 2, rCYP model); and $CLint_H$ scaled back from *in vivo* observed clearance values (model 3, retrograde model). Besides, we highlight a number of essential aspects regarding the design of the *in vitro* enzyme kinetic experiments and discuss the role of PBPK in the bottom-up scaling of these data to *in vivo* PK.

MATERIALS AND METHODS

Chemicals and Materials

All chemicals and reagents used were of the highest available grade: Na_2HPO_4, KH_2PO_4, KCl, $MgCl_2$, NADP, HCL (Merck, Darmstadt, Germany), glucose-6-phosphate, glucose-6-phosphate dehydrogenase (Roche Diagnostics GmbH, Manheim, Germany), Tramadol (TRC inc, Toronto, Canada), O-desmethyltramadol (ODT) (TRC inc, Toronto, Canada), N-desmethyltramadol (NDT) (LGC GmbH, Luckenwalde, Germany), N,O-didesmethyltramadol (NODT) (TRC inc, Toronto, Canada), O-desmethyltramadol-D6 (TRC inc, Toronto, Canada), ^{14}C-tramadol (Isotope Synthesis, Janssen).

Incubations with Human Liver Microsomes

A human liver microsomal pool (BD Biosciences, Woburn, USA), used for tramadol enzyme kinetics investigation, consisted of 50 adult donors and was stored at −80°C in an Ultra Freezer (New Brunswick scientific, Rotselaar, Belgium). Incubation mixtures (total volume 600 µl) consisted of 297 µl microsomal protein, 3 µl of a tramadol solution, and 300 µl cofactor mix containing an NADPH-regenerating system consisting of 1 mg of glucose-6-phosphate, 0.50 units of glucose-6-phosphate dehydrogenase, 0.25 mg of NADP and 1 mg of $MgCl_2.6H_2O$ in 1 ml of 0.5 M Na,K-phosphate buffer pH 7.4. Final microsomal protein concentrations ranged from 0.5 to 2 mg protein/ml. A preincubation with cofactor mix was done for 5 min in a shaking water bath at 37°C (100 oscillations/min) (Thermo, Waltham, USA). Incubations were started by adding 3 µl of a tramadol solution, resulting in a final concentration of 0.5, 1, 5, 20, 50, 100, 150, and 200 µM. Reactions were stopped at 2, 5, 7, 10, 20, and 30 min by transferring 100 µl aliquots into 96-well plates containing 10 µl ice-cold 4 N HCl and 10 µl of internal standard (O-desmethyltramadol-D6, 6 ng/ml). For each substrate and protein concentration level, samples were incubated in duplicate or triplicate and boiled control incubates were run in parallel to correct for non-enzymatic degradation. Ninety-six-well plates were then stored at −20°C waiting to be analyzed by UPLC-MS/MS.

Inhibition Assays with Human Liver Microsomes

Incubation mixtures were essentially the same as described above but relative volumes differed due to the addition of inhibitors, and contained 294 µl of microsomal protein, 300 µl of cofactor mix, 3 µl of inhibitor, and 3 µl of a tramadol solution. The final concentration of microsomal protein and tramadol in the incubations was 0.5 mg/ml and 1 µM, respectively. Inhibitors, which were dissolved in methanol in order to minimize solvent effects (0.5%), were ketoconazole (CYP3A inhibitor, 1 µM), SR-9186 (CYP3A4 inhibitor, 2.5 µM), quinidine (CYP2D6 inhibitor, 1 µM), and thioTEPA (CYP2B6 inhibitor, 10 µM). Incubations with the mechanism-based inhibitors SR-9186 and thioTEPA were equilibrated in a shaking water bath at 37°C (100 oscillations/min) (Thermo, Waltham, USA) for 5 and 15 min, respectively, and were then started by the addition of tramadol. A 5 min equilibration time was used for the reversible inhibitors ketoconazole and quinidine. All samples were stopped at 10 min in 96-well plates, containing 10 µl ice-cold 4 N HCl and 10 µl of internal standard. Linearity controls (incubation mixtures without inhibitors; tramadol 1 µM, 0.5 mg protein/ml, 10 min) as well as boiled controls were run in parallel to allow determination of the inhibited fraction and to correct for background, respectively. Ninety-six-well plates were then stored at −20°C waiting to be analyzed by UPLC-MS/MS.

Incubations with Recombinant CYP450 Enzymes

Supersomes™ are membrane fractions derived from baculovirus infected insect cells expressing a specific (selection of) drug metabolizing enzyme(s), i.e. CYP450 enzymes with or without NADPH cytochrome P450 reductase and cytochrome *b*5. Supersomes™ (BD Biosciences, Woburn, USA) were used in order to investigate the enzyme kinetic behavior of tramadol for the isolated CYPs. Incubation mixtures contained 297 µl of a given recombinant isoform at a final 100 pmol/ml (CYP isoform) concentration, together with 300 µl of the cofactor mix containing an NADPH-regenerating system (composition cfr "Materials and Methods" 2nd paragraph). These mixtures were preincubated in a shaking water bath at 37°C (100 oscillations/min) (Thermo, Waltham, USA) for 5 min and incubations were started by adding 3 µl of a tramadol solution. Tramadol final test concentrations were 1, 5, 150, and 250 µM. Reactions were stopped at 2, 5, 7, and 10 min by transferring 100 µl aliquots into 96-well plates containing 10 µl ice-cold 4 N HCl and 10 µl of internal standard. For each substrate and each recombinant isoform, samples were incubated in duplicate and Supersome™ insect controls, consisting of membrane fractions containing all proteins from the insect cell line except the CYP450 component, were run in parallel to correct for background. Ninety-six-well plates were then stored at −20°C waiting to be analyzed by UPLC-MS/MS.

Bioanalysis

Tramadol's main metabolites O-desmethyl tramadol (ODT, M1),N-desmethyl tramadol (NDT, M2), and N,O-didesmethyl tramadol (NODT, M5) (1) were quantified by a sensitive UPLC-MS/MS method. The Nexera UHPLC system (Shimadzu, Kyoto, Japan), consisting of a RackChanger

II, SIL-30 AC autosampler, CTO-30A column oven, and LC30AD pump units was linked *via* a Valco switching valve to an API 4000 QTRAP (AB Sciex, Toronto, Canada) equipped with a Turbo V™ ion source in ESI+ mode. For the chromatographic separation, a gradient was run—with solvents A (0.025 M ammonium acetate, pH 8.5) and B (acetonitrile:methanol 80:20, v/v)—from 5 to 50% B in 3 min, to 100% B in an immediate step gradient, held for 0.3 min, and back to 5% B, allowing 2 min re-equilibration, at a flow rate of 0.6 ml/min. The column was an Acquity UPLC BEH C18 1.7 μm 50×2.1 mm column (Waters, Milford, USA) packed with 1.7 μm particles and maintained at 60°C.

Metabolite formation was quantified by use of a calibrator set and quality control samples that were prepared by spiking 25 μl of reference standard solutions N-desmethyl tramadol (NDT), O-desmethyl tramadol (ODT), N,O-didesmethyl tramadol (NODT) containing O-desmethyltramadol-D6 as internal standard (6 ng/ml) to a mixture of 250 μl microsomal matrix and stopped with 25 μl 4 N HCl. Depending on the expected extent of metabolite formation ten calibrator levels (ranging 200-fold) and three QC levels (low, medium, high; made in duplicate) were selected for each analytical batch. Runs were accepted based on recommendations from the FDA's "Guidance for Industry–Bioanalytical Method Validation". At least four out of six QC samples were within 15% of their nominal value, for the calibration curve simple linear regression was applied with a weighting factor 1/x. Standards deviated not more than 15% from the nominal concentration, except for the LLOQ where 20% deviation was allowed. Samples in 96-well plates were thawed while shaking, submersed in an ultrasone bath, and centrifuged using an Allegra™ 25R ultracentrifuge (Beckman Coulter, Suarlée, Belgium). Depending on the expected degree of metabolite formation, between 1 and 10 μl supernatant was directly injected onto the column to assess concentrations of ODT, NDT, and NODT in the incubation samples.

Tramadol Enzyme Kinetics and IVIVE

Concentrations of metabolites in the incubation samples were corrected for protein concentration (mg microsomal protein/ml), reaction time (min), and initial substrate concentration (μM) in order to calculate the apparent *in vitro* clearance (CL_{app}) for every metabolite. CL_{app} was plotted *vs.* tramadol incubation concentration and a nonlinear model–with the model structure provided in equation 1–was fitted to the data, using the R statistics program (17). Models were evaluated by visually inspecting residual plots for bias. In equation 1 CL_{app} is the apparent *in vitro* clearance, expressed as μl/min/mg microsomal protein, v_o is the initial rate of metabolite formation in the incubate (pmol/min/mg protein), $[S]$ is tramadol concentration (μM), Km and $Vmax$ are the Michaelis-Menten constant (μM) and maximum velocity (pmol/min/mg protein), respectively. This equation allowed estimation of the parameters Km and Vmax, and hence the calculation of CLint.

$$CL_{app} = \frac{v_o}{[S]} = \frac{Vmax}{Km + [S]} \quad (1)$$

When the substrate concentration in the incubate is substantially below the Km (in practice [S] < Km/10), the intrinsic clearance (CLint) can be approximated from the ratio of Vmax/Km. When the substrate concentration is at Km, the CL_{app} approximates the half maximal CLint.

Tramadol incubation concentrations (0.5 to 250 μM) were chosen to be near the therapeutic plasma concentrations observed *in vivo* (C_{max} 2.25 μM (1)) in order to define the enzyme kinetic parameters of tramadol at a therapeutically relevant concentration test range. An unbound fraction in microsomes (fu_{mic}) of ~0.96 was estimated *in silico* using the prediction toolbox in Simcyp® V12.1 (18).

By scaling up an *in vitro* obtained (unbound) intrinsic clearance ($CLint_u$) with mechanistic information on the liver abundance of each CYP, the amount of microsomal protein per gram liver (MPPGL), and liver weight, a determination of the *in vivo* hepatic intrinsic clearance ($CLint_H$) can be obtained. Additionally, known variability in demographic and biological components is incorporated in order to predict drug disposition in relevant individuals with realistic variability. Additionally, for the scaling from recombinant systems, an intersystem extrapolation factor (ISEF) corrects for the inherent activity difference between recombinant systems and HLM (19,20).

Equations 2 and 3 are used for the mechanistic scaling of unbound intrinsic clearance to hepatic intrinsic clearance, obtained from HLM and recombinant systems, respectively. For scaling up HLM unbound CLint, the amount of microsomal protein per gram liver (MPPGL), and liver weight are needed to provide an estimate of the *in vivo* hepatic intrinsic clearance ($CLint_H$) (Eq. 2). For scaling up the unbound CLint determined from rCYP systems, the CYP450 isoform abundance *in vivo* and the ISEF value are additional factors needed to calculate the hepatic CLint (Eq. 3) (19).

$$CLint_H = CLint_{u,HLM} * MPPGL * g\ \ liver \quad (2)$$

$$CLint_H = CLint_{u,rCYP} * ISEF * [isoform]_{in\ \ vivo} * MPPGL * g\ \ liver \quad (3)$$

Subsequently, the hepatic intrinsic clearance ($CLint_H$) is integrated with the fraction unbound in plasma (fu_p), blood-to-plasma ratio (BP) and the hepatic blood flow (Q_H) in the commonly used well-stirred liver model in order to obtain an estimate of the hepatic plasma clearance (CL_H), as illustrated in Eq. 4:

$$CL_H = \frac{Q_H * fu_p * Clint_{\mathrm{H}}}{Q_H + fu_p * CLint_{\mathrm{H}}/BP} \quad (4)$$

Blood Distribution

The blood distribution of tramadol was investigated by incubating a tramadol concentration range (0.1–10 μM) in whole blood. Fresh whole blood was collected from three healthy male volunteers in EDTA-coated tubes to which ^{14}C-tramadol was spiked (no organic solvents were used). Spiked whole blood was left to equilibrate for 30 min in a shaking water bath Grant (type OLS200) (Grant instruments, Cambridge, UK) at 37°C and was gently homogenized every 10 min. After 30 min, three homogenous aliquots of 100 μl were pipetted to oxidation cups and the rest of the whole blood sample was centrifuged for 10 min at 1,700 g in a Hettich Rotixa (type 50S) (Hettich AG, Tuttlingen, Germany). Two aliquots of 100 μl plasma were placed in counting vials together with scintillation fluid Ultima Gold (PerkinElmer, Waltham, USA) and were counted by liquid scintillation counting (LSC) in a Tri-carb® 2900 TR (PerkinElmer, Waltham, USA). Whole blood samples were combusted in a Packard Sample Oxidizer 307 (PerkinElmer, Waltham, USA), released $^{14}CO_2$ was trapped with Carbosorb and mixed with scintillation fluid, and submitted to LSC. The radioactivity was measured in an aliquot of whole blood as well as in plasma from the same sample in order to assess the ratio of the whole blood concentration *vs.* the plasma concentration (blood-to-plasma or B:P ratio).

Simulations

An intravenous full PBPK model was selected in the Simcyp® Simulator V12.1 (Sheffield, UK) to predict pharmacokinetics as a function of time. In order to verify the simulations, PK parameters were compared to *in vivo* data (21–24).

The virtual clinical trial design was set to capture the pharmacokinetics as a function of time for a 100 mg tramadol iv bolus up to 24 h post-dose, in line with the *in vivo* observed AUC's which were also obtained from 0 to 24 h. Following molecular descriptors were extracted from literature and used as input for the PBPK model: molecular weight 264.4; logP 1.35; pKa 9.41; BP ratio 1.09 (own experiments); fu_p 0.8.

The virtual population was set to mimic the reference population in terms of the proportion male–female (30% female), the age range (23–57 years), and CYP2D6 metabolizer status (8.2% PM–86.5% EM–5.3% UM).

The distribution component of the PBPK model was represented by the Rodgers & Rowland model (method 2 in Simcyp®). The Rodgers and Rowland equation was used since this equation, in contrast to the Poulin and Theil equation (method 1 in Simcyp®), takes into account a tissue's acidic phospholipid fraction and takes explicit account of the extent of ionization of a compound at the pH of the compartment concerned. Since tramadol is almost completely ionized at pH 7.4, the Rodgers and Rowland equation will assume that binding to acidic phospholipids controls the distribution within the body (25). The elimination component of the PBPK model involved a renal and a hepatic clearance part. The renal plasma clearance was mechanistically predicted at 6.6 L/h (110 ml/min) using the permeability-limited mechanistic kidney model. Since this value was in good agreement with *in vivo* observations the renal clearance was fixed at 6.6 L/h for further simulations. The hepatic plasma clearance was investigated by means of an IVIVE-linked elimination model using kinetic data from *in vitro* experiments, further elaborated hereunder in the section "Hepatic clearance investigation". In addition, a sensitivity analysis was conducted to assess model robustness to changing input parameters other than CLint values, as well as a population simulation comparing the geometric means of clearance and volume of distribution and their associated variabilities with the reference data set used in this study (21–24).

Hepatic Clearance Investigation

The CYP-isoform specific CLint values that were used in the three different clearance modeling approaches, described hereunder, can be found in Table I. A factor of 1.58 was used to account for hepatic accumulation of the basic amine tramadol (see "Discussion" for details).

The HLM model (model 1) represents input from intrinsic clearance values obtained in HLM for the two main tramadol CYP-mediated metabolites ODT and NDT (Table II). The contribution of different CYP450 enzymes to the total intrinsic clearance per metabolite is estimated based on the effect of different chemical inhibitors (Table I). The rCYP model (model 2) consists of intrinsic clearance values obtained in isolated recombinant enzyme systems CYP3A4, 2D6, and 2B6 for the two main tramadol CYP450-mediated metabolites ODT and NDT (Table I). ISEF values for CYP3A4 and CYP2D6 were determined for scaling up tramadol rCYP450 kinetic data using probe substrates midazolam and dextromethorphan, respectively. CLint values for both probes were obtained in HLM as well as in rCYP systems, and specific CYP abundances of 137 and 8 pmol/mg microsomal protein were used to calculate the ISEF values for CYP3A4 and CYP2D6 (Table I), respectively (26,27). For CYP2B6, an ISEF-value of 0.43 was used as provided by Simcyp® V12.1. The retrograde model (model 3) calculates a retrograde hepatic intrinsic clearance per CYP isoform based on apparent *in vivo* CYP contributions in the total metabolism (Table I). Therefore, it can serve as a reference model next to the two other models in evaluating the prediction of the population

Table I Overall Summary of the CLint Values Obtained in Kinetic Experiments that were Used as Input for PBPK

Model	Formula	CYP isoform	CLint ODT[a]	CLint NDT[a]
1 HLM[b]	$CLint_{HLM}$ ($CLint_{ODT/NDT}$ * %CYP by chemical inhibition data)	3A4	0.12 (0.80*15%)	1.06 (1.63*65%)
		2D6	0.64 (0.80*80%)	0.08 (1.63*5%)
		2B6	0.04 (0.80*5%)	0.5 (1.63*30%)
2 rCYP[c]	$CLint_{rCYP}$ * ISEF	3A4	0.00 *0.23	0.11 *0.23
		2D6	0.57 *0.45	0.054 *0.45
		2B6	0.018 *0.43	0.20 *0.43
3 RG[d]	Retrograde model	2D6	48% of HepCL	
		3A4 + 2B6	52% of HepCL	

Specific CYP isoform contribution is incorporated through chemical inhibition (model 1) or ISEF values (model 2) or back-calculated from *in vivo* (model 3) for ODT and NDT

[a] CLint values for model 1 are expressed as μl/min/mg protein, whereas for model 2 CLint is expressed as μl/min/pmol CYP450

[b] Reported CLint values are obtained by multiplication of the $CLint_{HLM}$ values with % CYP isoform contribution calculated from inhibition assay data

[c] $CLint_{rCYP}$ obtained from recombinant enzyme systems, are presented with their specific ISEFs

[d] Retrograde model allows the user to set specific CYP contributions based on *in vivo* data in CYP2D6 PM and EM

clearance. Simulations were performed using a study design and healthy volunteer population that resembled the study design and covariate characteristics of the reference study, respectively (21–24). The simulations were executed using virtual populations of 1,000 subjects.

The CYP2D6 contribution in the current clearance models was assessed by comparing the fold increase in hepatic clearance between PM and EM with observed data from a study conducted by Pedersen *et al.* (28). Patients from this study were genotyped as *1/*1 (EM; n=8) and *4/*4 (n=7) or *4/*6 (PM) (n=1). The PBPK trial design was set to resemble the actual trial design as closely as possible by taking into account the actual age range, administered dose, proportion of male–female, and metabolizer phenotype in the two groups. One thousand virtual patients were simulated for every run.

Population Simulation

In Simcyp®, known covariates or correlations of different specifications of the population as well as the observed variability associated with each parameter involved in the bottom-up approach is considered to generate virtual subjects representative of those in the real world (10). Therefore, a population simulation was set up to investigate how well the three IVIVE-linked PBPK models could predict the population values of the clearance (CL) and volume of distribution (Vss) as well as their associated variability. In that respect the relative difference of the predicted and observed geometric means, calculated as (predicted-observed)/observed*100%, was used to compare the population values of CL and Vss. To compare the predicted and observed variability in the population, the fold difference of the predicted and observed coefficients of variation (CV) was used, assuming that these PK parameters follow log-normal distributions (Table III). Evaluation was based on visual inspection of observed and predicted 95% prediction intervals, calculated as suggested by Johnson *et al.* (29). The simulated virtual population consisted of 1,000 patients that mimicked the dosage, age range and male–female proportion of the reference studies (21–24).

Sensitivity Analysis

A sensitivity analysis was undertaken in order to define to what extent other input parameters than intrinsic clearance would influence the prediction of clearance (CL) using the clearance model 1 (based on HLM values) and volume of distribution (Vss) using the distribution model based on the Rodgers equations (25). Five input parameters of interest (logP, pKa, fraction unbound in plasma (fu), B:P ratio (BP), drug accumulation in hepatocyte (ACC)) were varied within the PBPK model (full factorial design (2^5)), using the Simcyp® Batch processor, between the lowest and the highest value published in literature or own experimental results. Following values (low level–high level) were used as input to the PBPK model:

Table II Overview of Enzyme Kinetic Parameters Km, Vmax and CLint and their Associated 95% Confidence Intervals for Tramadol's Two Main Metabolites ODT and NDT in Pooled HLM

	ODT	NDT
Km [95% CI] (μM)	57.5 [47.0; 71.1]	242 [174; 353]
Vmax [95% CI] (pmol/min/mg protein)	46.4 [38.9; 56.1]	395 [290; 565]
CLint [95% CI] (μl/min/mg protein)	0.80 [0.78; 0.84]	1.63 [1.57; 1.69]

Table III Hepatic Clearance Investigation by Comparison of three PBPK Models

	HLM model 1	rCYP model 2	Retrograde model 3
Renal involvement (%)	43	24	29
Hepatic involvement (%)	57	76	71
2D6 involvement in hepatic clearance (%)	29	29	44
2D6 involvement in total clearance (%)	17	22	31
Comparison of geometric mean and coefficient of variation			
Relative difference in geometric mean	−27%	+22%	+1%
Fold difference in CV	0.73	0.89	0.85
Hepatic clearance fold increase			
HepCL fold increase for CYP2D6 PM to EM	1.39	1.33	1.73[a]

First, the three models are presented with their renal, hepatic and 2D6 involvement, relative to the total clearance. Second, the 3 models are compared by their relative difference in geometric mean and fold of coefficients of variation (CV) *versus* observed data. Furthermore, the fold increase in hepatic clearance between CYP2D6 PM and EM is a measure of CYP2D6 contribution, indicating an underinvolvement of CYP2D6 in both the HLM and the rCYP model

[a] Observed hepatic clearance increase was calculated at 1.74 (27)

logP (1.35–2.41), pKa (9.14–9.44), fu (0.74–0.80), BP (1.09–1.20), ACC (1.5–3). The reason for varying the ACC factor 2-fold can be found in the discussion. PBPK simulations were performed using a healthy volunteer population that resembled the study population of the reference studies (21–24). One hundred virtual patients were simulated for every run. The prediction results were interpreted by means of a generalized linear model (glm) that was fitted to the PBPK prediction results, so as to disentangle the effects of the input parameters and their interactions on the prediction of CL and Vss.

RESULTS

In Vitro Results

CLint from HLM Assays

The metabolism kinetics of 0.5 μM to 250 μM tramadol to its two primary metabolites O-desmethyl tramadol (ODT) and N-desmethyl tramadol (NDT) was determined in pooled human liver microsomes. The secondary metabolite N,O-didesmethyl tramadol (NODT) was always about 1 and <3% of the amount of NDT and ODT formed, respectively, implying negligible underestimation of enzyme kinetic parameters due to secondary metabolism. Furthermore, preliminary experiments using ^{14}C-tramadol (data not shown) it was demonstrated that no other metabolites were formed than the ones described in this paper. The aim was to identify the intrinsic clearance for both metabolites at concentrations well below Km values, previously reported by Subrahmanyam *et al.* (2) (Km_{ODT} 116 μM; Km_{NDT} 1,021 μM). Linearity of metabolite formation to ODT and NDT in relation to time and protein content was investigated at 0.5 μM tramadol, and seemed to be linear up to 10 min and up to 1 mg of microsomal protein per ml.

Considering only linear kinetic data (initial velocities), the CL_{app} was calculated, as described in the previous section. The intrinsic clearance (CLint) is the apparent *in vitro* clearance that is maximal and constant at the lower end of the substrate concentration test range (illustrated for ODT and NDT in Fig. 2). Estimated enzyme kinetic parameters Km, Vmax, CLint are presented in Table II with their 95% confidence intervals.

HLM Inhibition Assays

Tramadol metabolism to ODT (Fig. 3, Table I) was found to be primarily inhibited (80%) by 1 μM quinidine, which causes a selective inhibition of CYP2D6 (30). Inhibition of another major CYP enzyme, CYP3A and CYP3A4 by ketoconazole and SR-9186 (31), respectively was derived to be approximately 15%. The rest of the ODT formation (5%) seemed to be mediated by CYP2B6 as indicated by the thioTEPA inhibitory effect.

Tramadol N-demethylation, displayed in Fig. 3 and Table I, is mainly mediated by CYP3A4 because about 60% of the metabolism to NDT is blocked by chemical inhibition with ketoconazole (1 μM) and SR-9186 (2.5 μM). The inhibitory effect of thioTEPA (10 μM) is believed to result from a dual effect on CYP3A4 and CYP2B6. This cross-reactivity was investigated by co-incubating tramadol with the two inhibitors. Knowing that SR-9186 causes selective inhibition of CYP3A4, the real contribution of CYP2B6 in the NDT formation can be estimated at 30% by subtracting the inhibition of SR-9186 alone from the inhibition with SR-9186 + thioTEPA, thereby correcting for thioTEPA's inhibitory effect on CYP3A4.

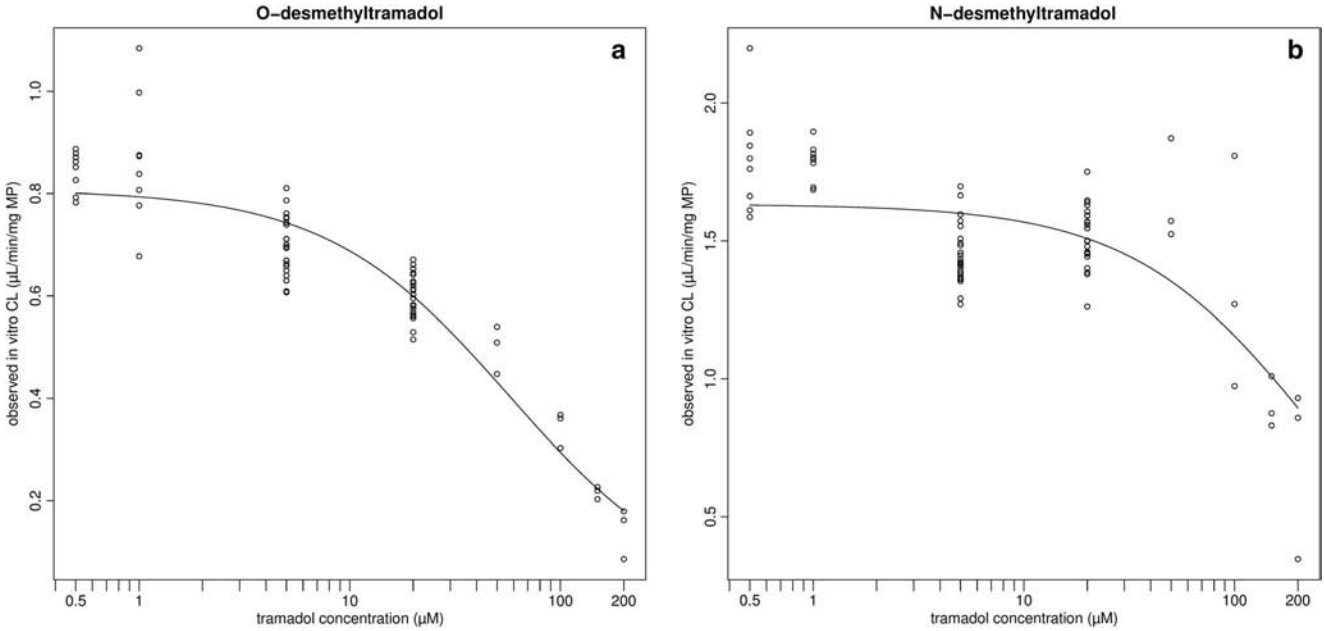

Fig. 2 The observed *in vitro* clearance (μL/min/mg microsomal protein) in relation to the incubation concentrations (μM) of tramadol for ODT (**a**) and NDT (**b**). For ODT the plateau of intrinsic clearance (CLint) is reached at 0.80 μl/min/mg protein, and for NDT the CLint was estimated at 1.63 μl/min/mg protein.

CLint from rCYP Assays

The kinetics of 1 µM to 250 µM tramadol to metabolites ODT and NDT was determined in recombinantly expressed enzyme systems containing CYP3A4, CYP2D6, CYP2B6, and insect controls (Supersomes™). Linear conditions were determined for both metabolites in relation to time per recombinant isoform at 100 pmol/ml. Enzymatic rates were linear up to 5 or 7 min, depending on the isoform under investigation. Only linear data should be used for calculation of the CL_{app}, yielding a plateau of CLint at tramadol concentrations well below Km (Fig. 4). CLint values that were used as input for hepatic clearance model 2, the rCYP model, can be found in Table I.

Blood Distribution

The blood distribution of tramadol appeared to be concentration independent within the test range of 0.1 to 10 µM tramadol and the blood-to-plasma ratio was determined at 1.09 (sd 0.02).

Simulation Results

Hepatic Clearance Investigation and Population Simulation

The involvement of the hepatic clearance in the total tramadol clearance was investigated by using the input from two distinct IVIVE-linked PBPK clearance models (HLM and rCYP model) and the retrograde clearance model as reference model. The results of this analysis are presented in Figs. 5, 6, and Table III. Input details for every clearance model are provided in the section "Materials and Methods"–"Simulations".

The HLM model as well as the rCYP model (models 1 and 2) are predicted within two fold of the observed geometric mean clearance, and the retrograde model, as a reference model, coincides with the geometric mean clearance (Fig. 5). From Table III it is apparent that the geometric mean clearance is slightly underpredicted in the HLM model but is somewhat overpredicted in the rCYP model. The variability in every model seems to be slightly underpredicted when compared to the observed variability. The CYP2D6 contribution, as illustrated by the fold increase of the hepatic clearance in PM *vs* EM (Table III), is underpredicted by both the HLM and the rCYP model, compared to the retrograde model and the observed data (28).

The steady-state volume of distribution was mechanistically predicted using the Rodgers and Rowland model. Preliminary simulations with the Poulin & Theil distribution model (32) resulted in a clear underprediction of the volume of distribution (data not shown). This is in line with previous reports on the better performing Rodgers & Rowland model, accounting for membrane interaction of ionized basic drugs (25,33), such as tramadol.

In Fig. 6 the three plots visualize the output from the simulation results by overlaying the *in vivo* observed clearances and PBPK predicted clearances in a plot per considered model. Circles represent data from *in vivo* studies by Lintz *et al.* and Quetglas *et al.* (21–24) with the dashed line being their overall geometric mean and the dotted line their 95%

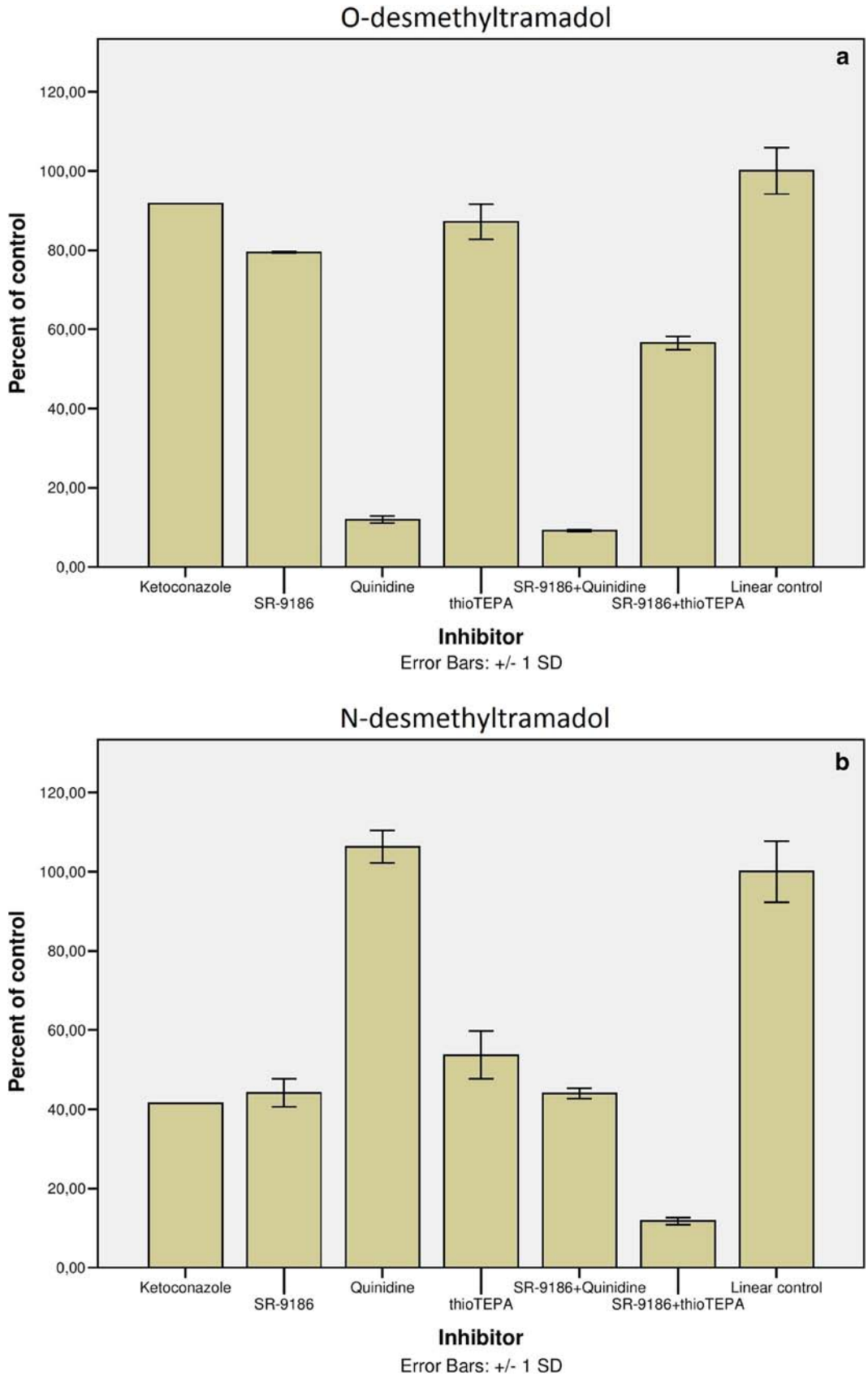

Fig. 3 The inhibition plot represents rest fractions of metabolite ODT (**a**) and NDT (**b**) in relation to inhibitor(s) present. A linear control was always run in parallel to the inhibition assays to determine 100% ODT and NDT formation.

prediction interval as calculated by Johnson (29). Y-axis represents total clearance for the predictions and observations, while the x-axis represents an index for the observations only -sorted per individual (Lintz data (21–23)) or per study population (Quetglas data (24))-. The greyed area represents the 95% prediction interval on the total clearance of the virtual population with its geometric mean as solid black line. Visually, the 95% prediction intervals for the rCYP and the retrograde model are more in line with the observed interval than for the HLM model, where an underestimation is present. In addition, Fig. 7 displays the observed and predicted values of Vss. Although some underprediction of the geometric mean Vss in this case is apparent, the predicted variability is in line with the observed one as can be concluded visually from the 95% prediction intervals.

Sensitivity Analysis

In order to identify those input parameters that significantly affected the PBPK prediction of total clearance (CL) and steady-state volume of distribution (Vss), a generalized linear model (glm) was fitted to the PBPK prediction outcomes. In this sensitivity analysis, effects of input parameters logP, pKa, fraction unbound in plasma (fu), blood:plasma ratio (BP), and hepatic accumulation (ACC) on PBPK predicted CL and Vss were determined. Isolated effects and interaction effects were distinguished in order to obtain meaningful parameter estimates (Table IV). It is worth noting that CL values were calculated as dose/AUC from Simcyp output sheets. This means that the predictions of CL in this case (PK profiles mode) are not independent from the prediction of Vss, because we record AUCs over the 24 h period post dose. In short, if input parameters that have an impact on the elimination or distribution of the drug are changed, plasma concentrations change, AUC_{0-24h} changes, and hence CL (=D/AUC_{0-24h}). The "(Intercept)" from the glm output displays the predicted total clearance (19.31 L/h) and volume of distribution (2.77 L/kg) when all five input parameters are at their lower level. Increasing the logP, fu, BP and ACC to their higher level, increases the predicted total clearance, while increasing pKa has a small but significantly lowering effect on the total clearance. An increase in logP and BP increases the predicted Vss, while increasing pKa and fu decreases the prediction of Vss. A simultaneous increase in both fu and ACC results in a higher predicted CL than what is to be expected from their isolated effects.

It can be concluded from the results in Table IV that based on the values for these five input parameters encountered in the literature or derived from own experimental work, the B:P ratio (BP) and the hepatic accumulation factor (ACC)

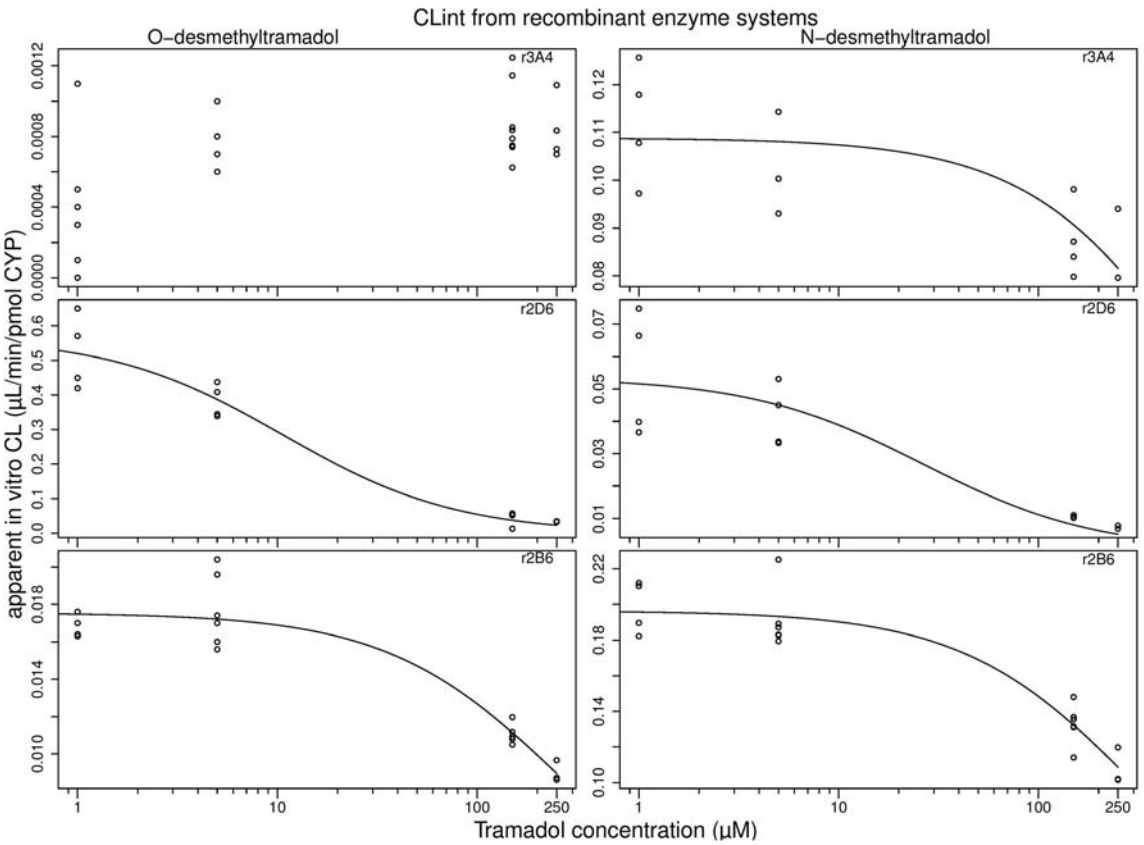

Fig. 4 The apparent *in vitro* clearance (µL/min/pmol CYP) for ODT and NDT in relation to the incubation concentrations (µM) of tramadol, for every recombinant enzyme CYP3A4, 2D6 and 2B6.

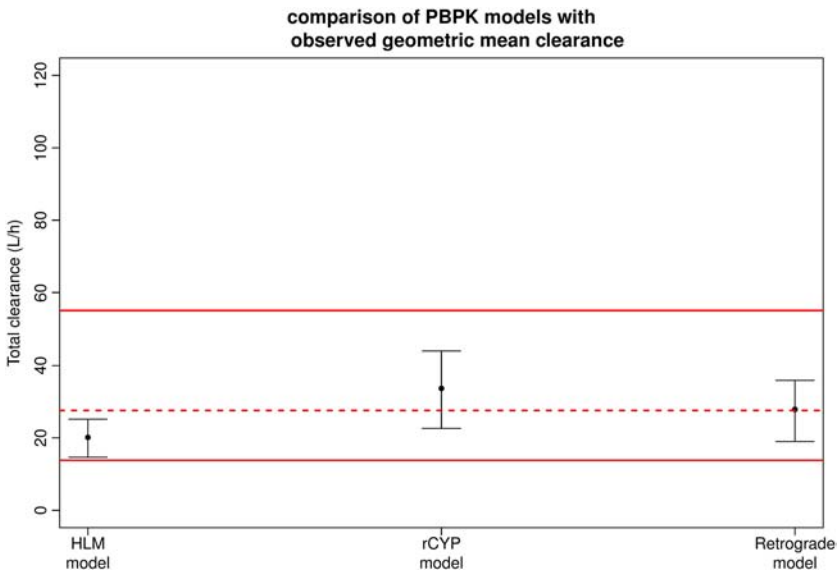

Fig. 5 The prediction of the total clearance per clearance model. *Black dots* are predicted geometric mean clearance and error bars represent the standard deviations. *Dashed* and *dotted lines* represent the observed geometric mean and their two fold boundaries, respectively. *HLM model* hepatic clearance model from human liver microsomes; *rCYP model* hepatic clearance model from recombinant human enzymes; *Retrograde model* hepatic clearance model from *in vivo* observed clearance data.

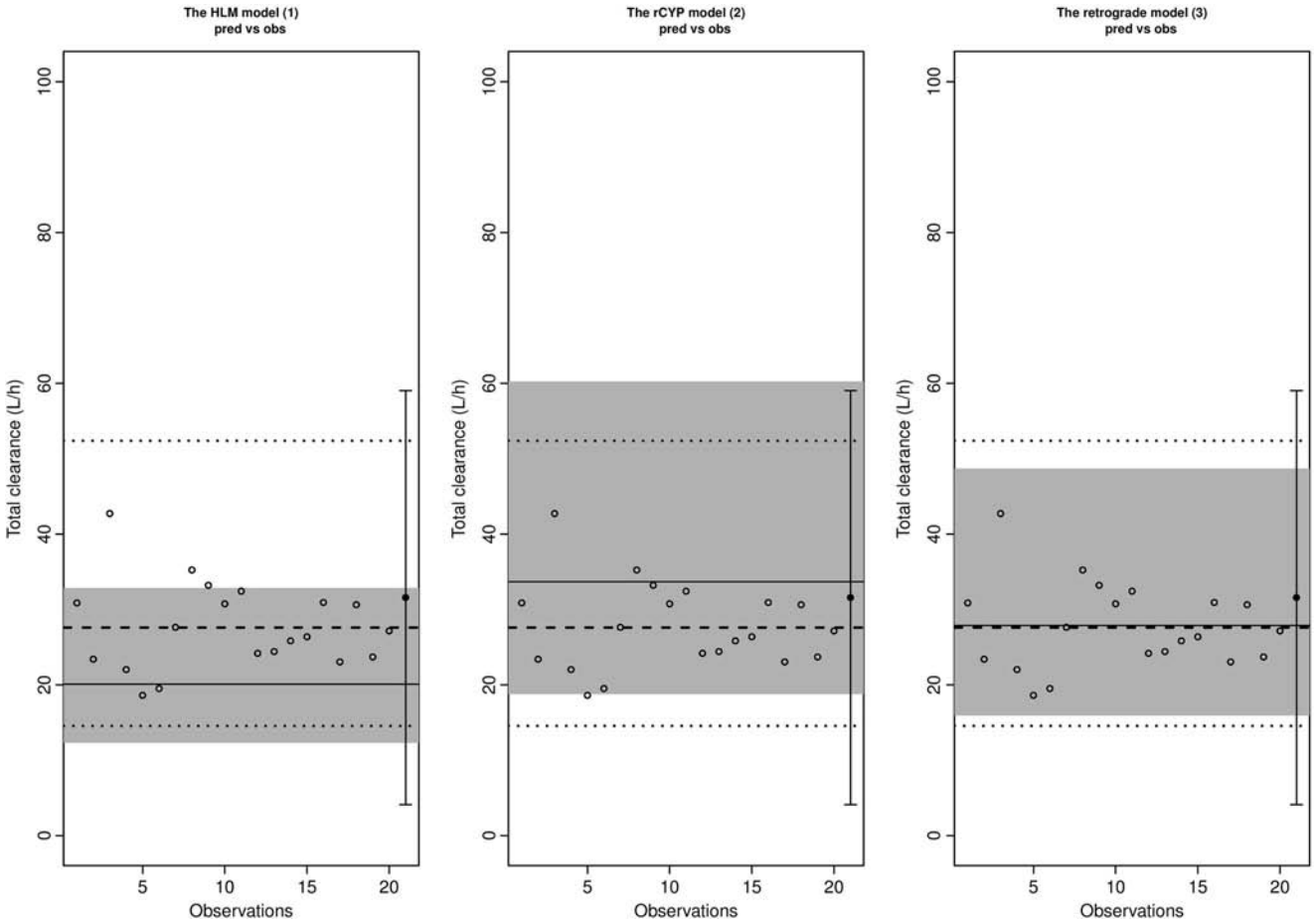

Fig. 6 Population simulation results for total clearance by the three models considered in this paper. *Open circles* (Lintz data (20–22)) and black circle (mean + − 2*sd) (Quetglas data (23)) represent data from *in vivo* studies with the dashed line being their overall geometric mean and the dotted line their 95% prediction interval. The greyed area represents the 95% prediction interval of the simulated population with its geometric mean as *solid black line*.

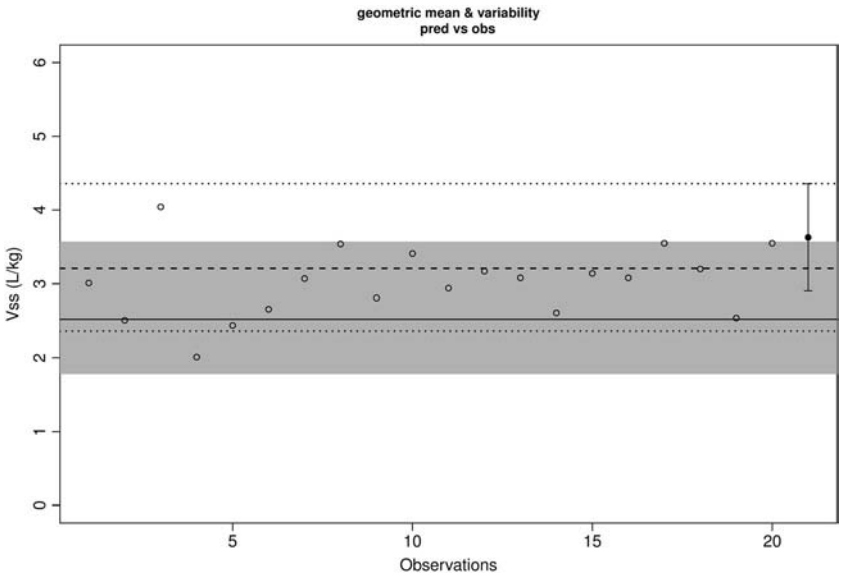

Fig. 7 Population simulation results for volume of distribution (Vss). Since we only considered one distribution model, only one plot is presented. *Open circles* (Lintz data (20–22)) and *black circle* (mean + − 2*sd) (Quetglas data (23)) represent data from *in vivo* studies with the dashed line being their overall geometric mean and the dotted line their 95% prediction interval. The greyed area represents the 95%prediction interval of the simulated population with its geometric mean as *solid black line*.

influenced the prediction of the total clearance most, while mainly the B:P ratio (BP) and the unbound fraction in plasma (fu) seemed to be affecting the value of Vss.

DISCUSSION

In this paper, we investigated the contribution of the hepatic clearance and the different CYP450 isoforms in the total clearance of tramadol by considering three different clearance models. Model 1 (HLM model) is based on data from HLM systems with specific CYP450 contributions *via* a chemical inhibition assay, while model 2 (rCYP model) uses recombinant *in vitro* clearance data with *ad hoc* determined ISEF values. Finally, model 3 (retrograde model) was included as a reference model, based on hepatic intrinsic clearances scaled back from *in vivo* hepatic clearance. For every model prediction not only the geometric mean of the total clearance but also the associated variability was evaluated. The difference in total clearance between these models is solely due to their hepatic component since renal clearance was fixed at 6.6 L/h. Apparently, the HLM model underpredicted the total clearance by −27%, while the rCYP model overpredicted the total clearance by +22% due to the fact that the hepatic clearance is increased in the rCYP model *vs* the HLM model (cfr Fig. 6 and Table III). The involvement of CYP2D6 still is underestimated in the HLM model and rCYP model, as can be concluded from the lower values for hepatic fold increase in Table III compared to the retrograde model. Although a large pool of human liver microsomes was used for the experiments, it has been previously shown that CYP2D6 is not the most stable isoform as could be derived from *in vitro* metabolism studies (34), and hence an underestimation of CYP2D6 activity as measured in this HLM batch could be a plausible explanation. Despite the fact that the rCYP model, based on study-specific ISEFs, somewhat overpredicts hepatic involvement, the CYP2D6 contribution is quite analogous to the one in the HLM model. Although an underprediction of −27% (HLM model) and an overprediction of +22% (rCYP model) of the total clearance is apparent, the question can be raised how much more accurate these bottom-up clearance models need to be. Are we only and unconditionally satisfied when the model predictions fall within the two fold prediction error margins? In our opinion, although our clearance model predictions clearly fall within these boundaries, there is undoubtedly room for improvement since a suboptimal CYP2D6 involvement in our clearance models prevails. Additional research should enable us to fine-tune these models further in their relative CYP contributions.

In the evaluation of the population simulations we found that the variability in all three models tends to be underpredicted, as is readily observed from the CV fold values being smaller than 1 in Table III. Upon visual inspection of Fig. 6 the variability of the rCYP model predictions seems larger than that of the HLM model predictions. However, when comparing the fold differences of CV between the two models, it is noticed that the difference between the fold differences (0.73 *vs* 0.89, Table III) is smaller than what would have been expected based on comparison of the 95% prediction intervals from the plots in Fig. 6. This indicates that variability, incorporated in the PBPK predictions, assumes a constant CV model. Having a good prior estimate of the

Table IV Sensitivity Analysis by a Generalized Linear Model (glm)

	Input level	Coefficients for CL (L/h)[a]		Coefficients for Vss (L/kg)[a]	
	Low–high	Estimate	Significance	Estimate	Significance
(Intercept)		19.31	***	2.77	***
logP	1.35–2.41	+0.19	***	+0.070	***
pKa	9.13–9.44	−0.020	**	−0.0075	***
fu	0.74–0.80	+0.025	**	−0.23	***
BP	1.09–1.20	±2.84	***	±1.12	***
ACC	1.5–3	±6.32	***	–	–
logP:pKa9.44		−0.098	***	−0.040	***
logP:fu0.8		–	–	+0.010	***
fu:BP1.2		−0.13	***	–	–
fu:ACC3		+0.49	***	–	–
BP:ACC3		−0.17	***	–	–
pKa:fu0.8		–	–	−0.0050	**
pKa:BP1.2		–	–	−0.0050	**

The isolated and interaction effects of input parameters on the geometric mean total clearance (CL) and volume of distribution (Vss) are displayed with significance level. (Intercept) has the value of the CL or Vss when all variables are at their lower input level. The estimate for a specific variable represents the increase/decrease in CL or Vss when this variable is changed to the higher input level

[a] Signif. codes '***' 0; '**' 0.001; '–' coefficient for this variable did not contribute significantly to the model

variability associated with the clearance through the use of PBPK modeling and simulation would definitely facilitate the prospective design and power calculations of an upcoming clinical trial.

In establishing *in vitro* intrinsic clearance values, using whatever *in vitro* system, it is well known that data should be linear with respect to time and protein concentration (35). Drug-specific HLM and recombinant enzyme kinetic data on tramadol are available in the literature (2). The data, however, are based on experiments using pools from five livers in which linearity was not investigated at the lowest *in vitro* test concentration. Moreover, the experiments were conducted at concentrations beyond those ever reached *in vivo* (intrahepatically). We therefore redesigned these experiments, in order to obtain physiologically relevant *in vitro* enzyme kinetic parameters. From the literature it was anticipated that tramadol would have a very low turnover *in vitro* (36), and our data equally substantiated that after 10 min incubation with 1 mg microsomal protein/ml, only 1% of tramadol at [S] < Km/10 was converted to its respective metabolites. By using appropriate, physiologically relevant incubation conditions, we were able to achieve quantitative estimates for the intrinsic clearances for both metabolites. Additionally, next to CYP2D6 and CYP3A4, a role for CYP2B6 of about 30% in the HLM metabolism of tramadol to NDT could be identified. This contribution however may be overemphasized due to the lower CYP2D6 activity present in this HLM batch. Nevertheless, in the case of CYP2D6 poor metabolizers e.g., the contribution of CYP2B6 and its expected associated variability (37) may become important covariates in the tramadol disposition.

An appealing feature of IVIVE-linked PBPK modeling and simulation is the learning-confirming principle, and consequently, the fact that mechanistic insights into the observed pharmacokinetics can be obtained (38). In that respect, the sensitivity analysis conducted in this case study clearly revealed that the B:P ratio and hepatic accumulation were factors most influential for the prediction of clearance, while the B:P ratio and fraction unbound in plasma strongly influenced the prediction of steady-state volume of distribution. While it is obvious why e.g. the hepatic accumulation and unbound fraction in plasma determine the prediction of the clearance and volume, respectively, it is not directly evident why the B:P ratio has such a marked effect, while logP and pKa hardly have any effect on the prediction of the tramadol clearance (Table IV). It has to be kept in mind however, that all predictions are based on kinetics as a function of time after a single iv dose, recording plasma concentrations up to 24 h post dose. Because B:P ratio, logP, and pKa all influence the prediction of the volume of distribution, and hence plasma concentrations, this has a rebound effect on the calculation of the clearance, calculated as dose/AUC_{0-24h}. The influence of the B:P ratio on the Vss was anticipated considering its role in the Rodgers & Rowland model for the prediction of tissue distribution (25). Therefore, a blood distribution experiment was conducted to ascertain the value of this B:P ratio in the model. Also, the positive effect of hepatic accumulation on the prediction of the hepatic clearance value proved to be

a very influential factor in this PBPK model, which is to be expected for low clearance drugs. Tramadol, as basic amine, is expected to accumulate inside the hepatocyte, solely driven by the existing pH gradient from 7.4 outside the cell, over 7.2 in the cytosol, to 5 in lysosomes (39). No transporters are thought to be involved in this process (6), which is in line with tramadol's BCS class I. An important issue in this matter is to establish which fraction of drug is available to the CYP450 enzyme system. The CLint, as determined *in vitro* in hepatocyte suspensions, should provide an indirect measure of the accumulation of unbound drug inside the hepatocyte, that is readily available for biotransformation. Nevertheless, a substantial underestimation of the CLint using hepatocyte incubations is a recognized problem (40,41) and questions concerning the presence of a comparable pH gradient in such an *in vitro* setup have arisen (42,43). Additionally, Poulin and co-workers also stated that the unbound drug fraction inside the hepatocyte could be greater than the unbound fraction in plasma because of binding effects of albumin on the hepatocyte cell surface *in vivo* on the one hand, and the aforementioned pH difference for ionizable compounds on the other hand. Consequently, by using *in vitro* systems in which these effects are unaccounted for, the CLint could be underestimated (44). Because of the inability to determine this uptake, a hepatic accumulation value of 1.58 (39) was used in all clearance models, based on the pH difference between the hepatocyte's outer (7.4) and inner (7.2) environment. To be able to put this into context, quite recently, equations were published by Berezhkovskiy *et al.* (42) that can be used to calculate an ionization factor, describing a drug's trapping behavior based on the drug's pKa and the pH difference over the hepatocyte membrane. These equations revealed that for tramadol by varying the intracellular pH between 7.0 and 7.2, the ionization factor takes on values of 1.67 and 2.5, respectively. In analogy, varying the hepatic accumulation factor 2-fold (from 1.5 to 3) in our sensitivity analysis increased prediction of the clearance with 33%. This indicates that small changes in pH can introduce significant changes in tissue-to-plasma concentration ratios. A better characterization of the relevant processes at hand could improve clearance prediction accuracy from an IVIVE perspective.

CONCLUSION

In conclusion, based on this work, we document that for quantitative PBPK modeling & simulation, all experiments to determine enzyme kinetic parameters should be performed with concentrations mimicking the *in vivo* obtained concentrations as closely as possible, while at the same time carefully scrutinizing reaction linearity. Tramadol as such displays a low turnover in hepatic *in vitro* systems, but using the physiological integration features of IVIVE-PBPK, i.e. the combination with a high fraction unbound in plasma (80%) and the hepatic accumulation (1.58 fold) of tramadol, leads to a simulation result corresponding with the quite extensive metabolism (approximately 80% of dose) observed *in vivo*. Three distinct clearance models were described in this paper. The HLM model slightly underpredicted, while the rCYP model slightly overpredicted the geometric mean clearance. The CYP2D6 contribution was underpredicted in both cases. Although the variability also suffered from some underpredicition, the predicted coefficients of variation were in line with observed ones. We clearly illustrated that the use of a retrograde model as reference model facilitates the bottom-up PBPK model building process. The IVIVE-linked PBPK approach has proven to be a very useful tool in integrating available *in vitro*, *in silico*, and *in vivo* data on tramadol to successfully predict the *in vivo* PK and gain mechanistic insight in relevant disposition covariates at hand.

ACKNOWLEDGMENTS AND DISCLOSURES

Karel Allegaert is supported by the Fund for Scientific Research, Flanders (Fundamental Clinical Investigatorship 1800214N).

REFERENCES

1. Grond S. Clinical pharmacology of tramadol. Clin Pharmacokinet. 2004;43(13):879–923.
2. Subrahmanyam V, Renwick AB, Walters DG, Young PJ, Price RJ, Tonelli AP, *et al.* Identification of cytochrome P-450 isoforms responsible for cis-tramadol metabolism in human liver microsomes. Drug Metab Dispos. 2001;29(8):1146–55.
3. Whirl-Carrillo M, McDonagh EM, Hebert JM, Gong L, Sangkuhl K, Thorn CF, *et al.* Pharmacogenomics knowledge for personalized medicine. Clin Pharmacol Ther. 2012;92(4):414–7.
4. Gonzalez F, Tukey R. Drug metabolism. In: Goodman L, Gilman A, Brunton L, Lazo J, Parker K, editors. Goodman and Gilman's the pharmacological basis of therapeutics. New York: McGraw Hill; 2006. p. 71–91.
5. Zhou SF. Polymorphism of human cytochrome P450 2D6 and its clinical significance: part I. Clin Pharmacokinet. 2009;48(11):689–723.
6. Tzvetkov MV, Saadatmand AR, Lotsch J, Tegeder I, Stingl JC, Brockmoller J. Genetically polymorphic OCT1: another piece in the puzzle of the variable pharmacokinetics and pharmacodynamics of the opioidergic drug tramadol. Clin Pharmacol Ther. 2011;90(1):143–50.
7. Stamer UM, Musshoff F, Kobilay M, Madea B, Hoeft A, Stuber F. Concentrations of tramadol and O-desmethyltramadol enantiomers in different CYP2D6 genotypes. Clin Pharmacol Ther. 2007;82(1):41–7.
8. Rowland M, Peck C, Tucker G. Physiologically-based pharmacokinetics in drug development and regulatory science. Annu Rev Pharmacol Toxicol. 2011;51(1):45–73.
9. Edginton AN, Theil FP, Schmitt W, Willmann S. Whole body physiologically-based pharmacokinetic models: their use in clinical drug development. Expert Opin Drug Metab Toxicol. 2008;4(9):1143–52.
10. Jamei M, Marciniak S, Feng K, Barnett A, Tucker G, Rostami-Hodjegan A. The Simcyp population-based ADME simulator. Expert Opin Drug Metab Toxicol. 2009;5(2):211–23.

11. De Bock L, Colin P, Boussery K, Van Bocxlaer J. Development and validation of an enzyme-linked immunosorbent assay for the quantification of cytochrome 3A4 in human liver microsomes. Talanta. 2012;99:357–62.
12. Bouzom F, Walther B. Pharmacokinetic predictions in children by using the physiologically based pharmacokinetic modelling. Fundam Clin Pharmacol. 2008;22(6):579–87.
13. Rostami-Hodjegan A. Physiologically based pharmacokinetics joined with in vitro-in vivo extrapolation of ADME: a marriage under the arch of systems pharmacology. Clin Pharmacol Ther. 2012;92(1):50–61.
14. Obach RS, Reed-Hagen AE. Measurement of Michaelis constants for cytochrome P450-mediated biotransformation reactions using a substrate depletion approach. Drug Metab Dispos. 2002;30(7):831–7.
15. Di L, Atkinson K, Orozco CC, Funk C, Zhang H, McDonald TS, *et al.* In vitro-in vivo correlation for low-clearance compounds using hepatocyte relay method. Drug Metab Dispos. 2013;41(12):2018–23.
16. Fagerholm U. Prediction of human pharmacokinetics-evaluation of methods for prediction of hepatic metabolic clearance. J Pharm Pharmacol. 2007;59(6):803–28.
17. R Core Team. R. A language and environment for statistical computing. Vienna: R Foundation for Statistical Computing; 2013.
18. Turner D, Rostami-Hodjegan A, Tucker G, Yeo K. Prediction of nonspecific hepatic microsomal binding from readily available physicochemical properties. Drug Metab Rev. 2007;38(S1):162.
19. Crewe HK. Are there differences in the catalytic activity per unit enzyme of recombinantly expressed and human liver microsomal cytochrome P450 2C9? A systematic investigation into inter-system extrapolation factors. Biopharm Drug Dispos. 2011;32(6):303–18.
20. Rostami-Hodjegan A, Tucker GT. Simulation and prediction of in vivo drug metabolism in human populations from in vitro data. Nat Rev Drug Discov. 2007;6(2):140–8.
21. Lintz W, Barth H, Osterloh G, Schmidt-Bothelt E. Bioavailability of enteral formulations 1st communication: capsules. Arzneimittelforschung. 1986;36–2(8):1278–83.
22. Lintz W, Barth H, Becker R, Frankus E, Schmidt-Bothelt E. Pharmacokinetics of tramadol and bioavailability of enteral tramadol formulations—2nd communication: drops with ethanol. Arzneimittelforschung. 1998;48(5):436–45.
23. Lintz W, Barth H, Osterloh G, Schmidt-Bothelt E. Pharmacokinetics of tramadol and bioavailability of enteral tramadol formulations—3rd communication: suppositories. Arzneimittelforschung. 1998;48(9):889–99.
24. Quetglas EG, Azanza JR, Cardenas E, Sadaba B, Campanero MA. Stereoselective pharmacokinetic analysis of tramadol and its main phase I metabolites in healthy subjects after intravenous and oral administration of racemic tramadol. Biopharm Drug Dispos. 2007;28(1):19–33.
25. Rodgers T, Leahy D, Rowland M. Physiologically based pharmacokinetic modeling 1: predicting the tissue distribution of moderate-to-strong bases. J Pharm Sci. 2005;94(6):1259–76.
26. Chen Y, Liu L, Nguyen K, Fretland AJ. Utility of intersystem extrapolation factors in early reaction phenotyping and the quantitative extrapolation of human liver microsomal intrinsic clearance using recombinant cytochromes P450. Drug Metab Dispos. 2011;39(3):373–82.
27. Yeo KR. Abundance of cytochromes P450 in human liver: a meta-analysis. Br J Clin Pharmacol. 2004;57(5):687–8.
28. Pedersen RS, Damkier P, Brosen K. Enantioselective pharmacokinetics of tramadol in CYP2D6 extensive and poor metabolizers. Eur J Clin Pharmacol. 2006;62(7):513–21.
29. Johnson TN, Rostami-Hodjegan A, Tucker GT. Prediction of the clearance of eleven drugs and associated variability in neonates, infants and children. Clin Pharmacokinet. 2006;45(9):931–56.
30. von Moltke LL, Greenblatt DJ, Duan SX, Daily JP, Harmatz JS, Shader RI. Inhibition of desipramine hydroxylation (cytochrome P450-2D6) in vitro by quinidine and by viral protease inhibitors: relation to drug interactions in vivo. J Pharm Sci. 1998;87(10):1184–9.
31. Li X, Song X, Kamenecka TM, Cameron MD. Discovery of a highly selective CYP3A4 inhibitor suitable for reaction phenotyping studies and differentiation of CYP3A4 and CYP3A5. Drug Metab Dispos. 2012;40(9):1803–9.
32. Poulin P, Theil FP. Prediction of pharmacokinetics prior to in vivo studies. 1. Mechanism-based prediction of volume of distribution. J Pharm Sci. 2002;91(1):129–56.
33. De Buck SS, Mackie CE. Physiologically based approaches towards the prediction of pharmacokinetics: in vitro-in vivo extrapolation. Expert Opin Drug Metab Toxicol. 2007;3(6):865–78.
34. Foti RS, Fisher MB. Impact of incubation conditions on bufuralol human clearance predictions: enzyme liability and nonspecific binding. Drug Metab Dispos. 2004;32(3):295–304.
35. Sjogren E, Nyberg J, Magnusson MO, Lennernas H, Hooker A, Bredberg U. Optimal experimental design for assessment of enzyme kinetics in a drug discovery screening environment. Drug Metab Dispos. 2011;39(5):858–63.
36. Shao L, Hewitt M, Jerussi TP, Wu F, Malcolm S, Grover P, *et al.* In vitro and in vivo evaluation of O-alkyl derivatives of tramadol. Bioorg Med Chem Lett. 2008;18(5):1674–80.
37. Zhang H, Sridar C, Kenaan C, Amunugama H, Ballou DP, Hollenberg PF. Polymorphic variants of cytochrome P450 2B6 (CYP2B6.4-CYP2B6.9) exhibit altered rates of metabolism for bupropion and efavirenz: a charge-reversal mutation in the K139E variant (CYP2B6.8) impairs formation of a functional cytochrome P450-reductase complex. J Pharmacol Exp Ther. 2011;338(3):803–9.
38. Zhao P, Zhang L, Grillo JA, Liu Q, Bullock JM, Moon YJ, *et al.* Applications of physiologically based pharmacokinetic (PBPK) modeling and simulation during regulatory review. Clin Pharmacol Ther. 2011;89(2):259–67.
39. Hallifax D, Houston JB. Saturable uptake of lipophilic amine drugs into isolated hepatocytes: mechanisms and consequences for quantitative clearance prediction. Drug Metab Dispos. 2007;35(8):1325–32.
40. Ito K, Houston JB. Comparison of the use of liver models for predicting drug clearance using in vitro kinetic data from hepatic microsomes and isolated hepatocytes. Pharm Res. 2004;21(5):785–92.
41. Foster JA, Houston JB, Hallifax D. Comparison of intrinsic clearances in human liver microsomes and suspended hepatocytes from the same donor livers: clearance-dependent relationship and implications for prediction of in vivo clearance. Xenobiotica. 2011;41(2):124–36.
42. Berezhkovskiy LM, Liu N, Halladay JS. Consistency of the novel equations for determination of hepatic clearance and drug time course in liver that account for the difference in drug ionization in extracellular and intracellular tissue water. J Pharm Sci. 2012;101(2):516–8.
43. Berezhkovskiy L, Wong S, Halladay J. On the maintenance of hepatocyte intracellular pH 7.0 in the in-vitro metabolic stability assay. J Pharmacokinet Pharmacodyn. 2013;40(6):683–9.
44. Poulin P, Hop CECA, Ho Q, Halladay JS, Haddad S, Kenny JR. Comparative assessment of in vitro-in vivo extrapolation methods used for predicting hepatic metabolic clearance of drugs. J Pharm Sci. 2012;101(11):4308–26.